JACS
JOURNAL OF THE AMERICAN CHEMICAL SOCIETY
Communication
pubs.acs.org/JACS

Relative Binding Free Energies of Adenine and Guanine to Damaged and Undamaged DNA in Human DNA Polymerase η: Clues for Fidelity and Overall Efficiency

Melek N. Ucisik and Sharon Hammes-Schiffer*

Department of Chemistry, University of Illinois at Urbana—Champaign, 600 South Mathews Avenue, Urbana, Illinois 61801-3364, United States

Supporting Information

ABSTRACT: Human DNA polymerase η (Pol η) plays an essential protective role against skin cancer caused by cyclobutane thymine−thymine dimers (TTDs), a frequent form of DNA damage arising from exposure to the sun. This enzyme rescues stalled replication forks at the TTDs by inserting bases opposite these DNA defects. Herein we calculate binding free energies for a free deoxyribose nucleotide triphosphate, dATP or dGTP, to Pol η complexed with undamaged or damaged DNA. The calculations indicate that the binding of dATP to the enzyme−DNA complex is thermodynamically favored for TTD-containing DNA over undamaged DNA, most likely because of more extensive hydrogen-bonding interactions between the TTD and the enzyme that hold the TTD more rigidly in place. The calculations also illustrate that dATP binding is thermodynamically favored over dGTP binding at both thymine positions of the TTD, most likely due to more persistent and stable hydrogen-bonding interactions between the TTD and dATP than between the TTD and dGTP. This free energy difference is slightly greater for binding at the 5′ thymine position than at the 3′ thymine position, presumably because of stabilization arising from the A:T base pair formed at the 3′ position of the TTD in the previous step of Pol η function. All of these trends in binding free energies are consistent with experimental measurements of binding strength, fidelity, processivity, and overall efficiency. The insights gained from this analysis have implications for drug design efforts aimed at modifying the binding properties of this enzyme for improving cancer chemotherapy treatments.

The enzyme DNA polymerase η (Pol η) is vital for human skin cells to survive the ultraviolet (UV) damage from daily exposure to the sun.[1,2] Mutations of the gene that encodes this enzyme result in the variant form of Xeroderma Pigmentosum, a condition characterized by intolerance to UV-induced skin damage and high predisposition to skin cancer.[3] Pol η is responsible for DNA replication at sites of cyclobutane thymine−thymine dimers (TTDs), the most frequent form of UV-induced DNA damage, where the replication fork stalls due to the inability of replicative DNA polymerases α, δ, and ε to handle these defective regions.[4,5] In particular, the role of Pol η is to extend the DNA primer strand by inserting bases opposite such DNA defects during replication, a process called translesion synthesis.[6] Pol η performs this process with relatively high accuracy and processivity at lesion sites,[7,8] whereas its fidelity and overall efficiency are lowered when operating on undamaged DNA.[9] Pol η also performs effective translesion synthesis at sites of cisplatin, gemcitabine, and oxaliplatin DNA adducts, products of commonly used anticancer therapies, diminishing the potency of such chemotherapy.[10−12] Hence, understanding the basis for its selectivity and processivity is important for discerning how its interference with cancer therapy could be prevented. In particular, clarification of the binding properties of the Pol η−DNA system could assist in the design of inhibitors to prevent this interference.

We performed binding free energy simulations to shed light on the molecular basis of the fidelity and efficiency of Pol η. Specifically, we used thermodynamic integration (TI)[13] to calculate the relative binding free energies[14−20] of deoxyadenosine triphosphate (dATP) binding to the TTD versus two undamaged thymines and of dATP versus deoxyguanosine triphosphate (dGTP) binding to the TTD. The results are justified via analysis of hydrogen-bonding interactions, thereby

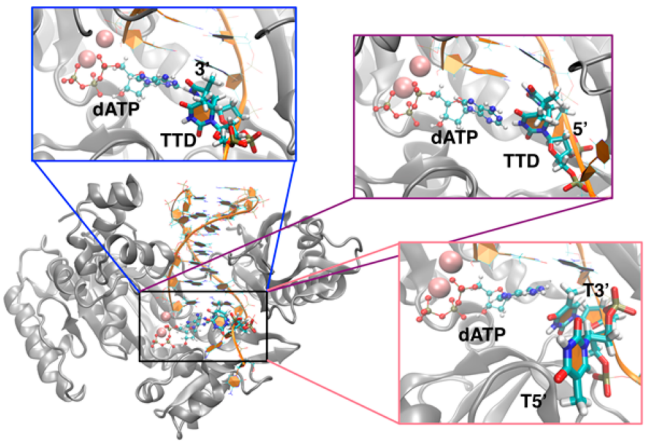

Figure 1. Catalytic region of Pol η (lower left) complexed with a DNA template/primer and a free dNTP. The black rectangle surrounds the active site of the enzyme, and three different active sites are magnified in colored rectangles with the TTD or TT depicted in licorice and dATP shown in ball-and-stick. A fourth system was also simulated where the active site shown in the blue box featured a dGTP instead of a dATP.

Received: August 10, 2015
Published: October 4, 2015

DOI: 10.1021/jacs.5b08451
J. Am. Chem. Soc. 2015, 137, 13240−13243

also elucidating fundamental binding characteristics of this system.[21] Previously we propagated multiple microsecond molecular dynamics (MD) trajectories for four systems, each including the catalytic domain of Pol η, a DNA template/primer containing either a TTD or two undamaged thymines (TT), and either dATP or dGTP as the free base (Figure 1 and Supporting Information, Table S1). We found that the structures and equilibrium dynamics of the four systems studied were similar in most aspects except for certain differences in hydrogen-bonding interactions between the DNA constructs and the enzyme.[22] Analysis of these hydrogen-bonding interactions in the context of the binding free energy calculations provides insight into the molecular basis for the experimentally observed fidelity and overall efficiency. Note that this analysis focuses on thermodynamic aspects and does not address kinetic aspects that may also impact fidelity and overall efficiency.

The objective of our TI simulations was to address three questions regarding the relative binding free energies of the dNTP (N = A or G) to the Pol η–DNA complex. First, is the binding of dATP to an enzyme–DNA complex containing the TTD more thermodynamically favorable than the binding of dATP to a complex with undamaged DNA? Second, is the binding of dATP at the 3′ T of the TTD in damaged DNA more thermodynamically favorable than the binding of dGTP at the same site? Third, is the binding of dATP at the 5′ T of the TTD in damaged DNA more thermodynamically favorable than the binding of dGTP at the same site?

The three thermodynamic cycles used to address these questions are depicted in Scheme 1. The first thermodynamic

Scheme 1. Thermodynamic Cycles Examining the Binding of (a) dATP to TTD-Containing DNA versus Undamaged DNA, (b) dATP versus dGTP to 3′ T of the TTD, and (c) dATP versus dGTP to 5′ T of the TTD

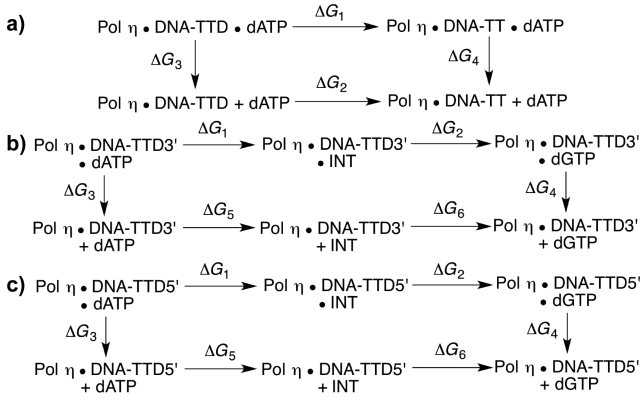

cycle, denoted TTDvsTT, describes the transformation of a TTD to two undamaged thymines when interacting with dATP and Pol η. The second cycle, denoted AvsG3′, describes the conversion of dATP to dGTP when interacting with the 3′ T of the TTD through a fictitious intermediate (Figure S1) designed to facilitate conformational sampling and convergence. Finally, the third cycle, denoted AvsG5′, examines the same conversion as does the second cycle except the dNTP interacts with the 5′ T of the TTD. Each of these three cycles addresses one of the three questions above in sequential order. The TI calculations[23−25] utilized the pmemd implementation of alchemical transformations[26] in the AMBER 14 suite of programs.[27] In TI, the transformation between two related systems occurs in a series of steps controlled by the coupling parameter λ, which ranges from 0 to 1. For each discrete λ, an MD trajectory is propagated to sample $dV/d\lambda$, the derivative of the potential energy with respect to λ. The free energy difference between these two systems is calculated by integrating the average of $dV/d\lambda$ over λ. A complete protocol is given in the Supporting Information.

Pol η has been shown experimentally to bind the TTD-containing DNA more strongly than undamaged DNA.[7,8,28] Moreover, Pol η was found to exhibit lower processivity for undamaged DNA, which could reflect different binding free energies for dATP to the enzyme–DNA complex with and without the TTD.[8,29] On the basis of the TI calculations for the TTDvsTT thermodynamic cycle (Scheme 1a), we calculated the relative binding free energy of dATP to the enzyme–DNA complex with and without the TTD to be -4.3 ± 1.0 kcal/mol, favoring the binding of dATP to the enzyme–DNA complex with the TTD. The data for the five independent TI calculations are provided in Table S2 and Figure S2. This calculated relative binding free energy is consistent with the experimental finding of higher processivity for TTD-containing DNA than undamaged DNA. As shown by analysis of our previous microsecond MD trajectories,[22] the extent of hydrogen-bonding interactions with the enzyme and the dATP is significantly greater for the TTD than for the two undamaged thymines. The more extensive hydrogen-bonding interactions between the TTD and the environment holds the TTD more rigidly in place, leading to a more specific and consistent orientation of the lesion opposite the dATP, which could facilitate the tighter binding of dATP (Figure 2). The root-mean-square deviation analysis performed on the TTD or the TT motif for each system supports this finding (Figure S3). Moreover, the average root-mean-square fluctuation was found to be 0.5 Å for the TTD and 1.0 Å for the normal TT motif in the microsecond MD trajectories, indicating greater mobility for the TT motif.

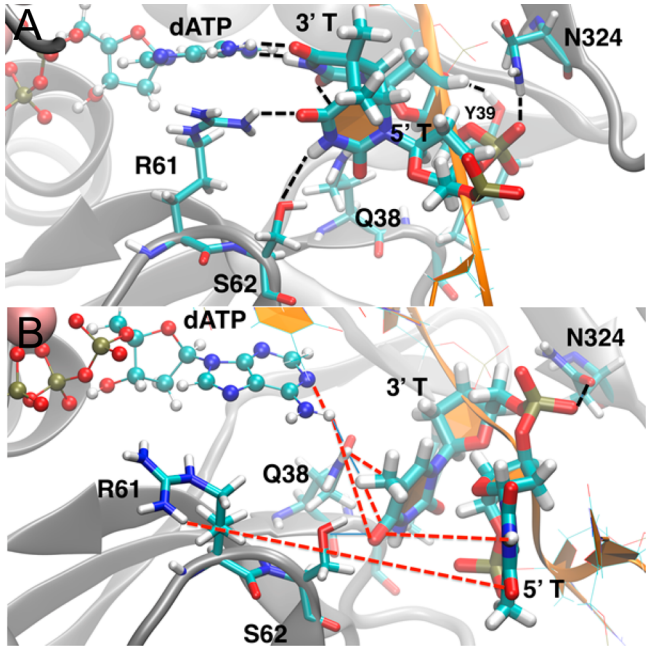

Figure 2. (A) Hydrogen bonds around the TTD lesion, indicated by black dashed lines. Our MD studies highlighted Q38, Y39, R61, S62, N324, and dATP as important hydrogen-bonding partners for the TTD. (B) The two undamaged thymines at the same location lack most of these hydrogen-bonding interactions, which are indicated by red dashed lines.

DOI: 10.1021/jacs.5b08451
J. Am. Chem. Soc. 2015, 137, 13240−13243

The low fidelity of Pol η[7−9] compared to general polymerases is related to the misincorporation ratio of dNTPs other than dATP, in particular dGTP instead of dATP opposite the 3′ and 5′ thymine positions of a TTD. Experimentally, the rate of dGTP incorporation opposite a thymine in undamaged DNA by Pol η was found to be 1/18; i.e., one of every 18 inserted dNTP molecules is erroneously a dGTP, which is a high error rate in comparison to other replicative DNA polymerases.[9] This ratio decreases to 1/26 opposite the 3′ T of the TTD in damaged DNA.[8] On the other hand, experiments indicate that Pol η binds dATP more strongly than dGTP. The K_M values measured in these experiments were significantly lower for dATP insertion compared to dGTP insertion with both TTD-containing and undamaged DNA templates, although the difference in K_M values was more pronounced in the presence of a TTD.[9,28,30] Our TI calculations for the AvsG3′ thermodynamic cycle (Scheme 1b) indicate that the relative binding free energy of dATP versus dGTP at the 3′ T of the TTD is −2.4 ± 1.1 kcal/mol, favoring dATP over dGTP binding. The data for the five independent TI calculations are provided in Table S3 and Figure S4. This binding free energy is consistent with the experimental observation of stronger binding of dATP versus dGTP. Moreover, the finding that this free energy difference is relatively small provides a plausible explanation for the experimentally measured high misincorporation rate of dGTP.

In our previous analysis of microsecond MD trajectories,[22] we did not observe any significant differences between dGTP and dATP interactions with the enzyme.[22] The present work focuses on hydrogen-bonding interactions between dNTP and the TTD. This analysis reveals differences between the base pairing of dATP versus dGTP with the TTD. The usual A:T Watson−Crick hydrogen-bonding interactions are detected in the vast majority of the saved configurations in the MD trajectories with dATP at the 3′ T of the TTD. The hydrogen bond between the N3 amino hydrogen of the 3′ T of the TTD and the N1 of the adenine of dATP is observed in 97% of all saved configurations with an average donor−acceptor distance of 3.0 Å and an average donor−hydrogen−acceptor angle of 163°. The O4 of the 3′ T of the TTD exhibits a hydrogen bond with one of the N6 amino hydrogens in dATP in 87% of the saved configurations with an average donor−acceptor distance of 3.0 Å and an average donor−hydrogen−acceptor angle of 160°. When dATP is replaced with dGTP, this persistent and stable base-pairing interaction is no longer observed. The most frequent hydrogen-bonding interaction between dGTP and the 3′ T of the TTD involves the O6 atom of the guanine and the N3 hydrogen of the thymine. This hydrogen bond is observed in 61% of the saved configurations with an average donor−acceptor distance of 2.9 Å and an average donor−hydrogen−acceptor angle of 156°. A second hydrogen-bonding interaction is formed between the N1 hydrogen of the guanine and the O2 atom of the thymine in 54% of the saved configurations with an average donor−acceptor distance of 3.0 Å and an average donor−hydrogen−acceptor angle of 153°. These base-pairing interactions are depicted in Figure 3. This T:G wobble base pair was also observed in previous crystal structures.[31] The diminished base-pairing interactions for dGTP compared to dATP may be the underlying reason for the stronger binding of dATP compared to dGTP.

Experimental studies indicate that the mis-incorporation rate of dGTP instead of dATP is different when the dNTP is opposite the 3′ T versus the 5′ T within the TTD.[30] Specifically, the error rate of T:G mismatches at the 5′ T of the TTD was found to be 12 times lower than at the 3′ T.[8] The difference in the error rates

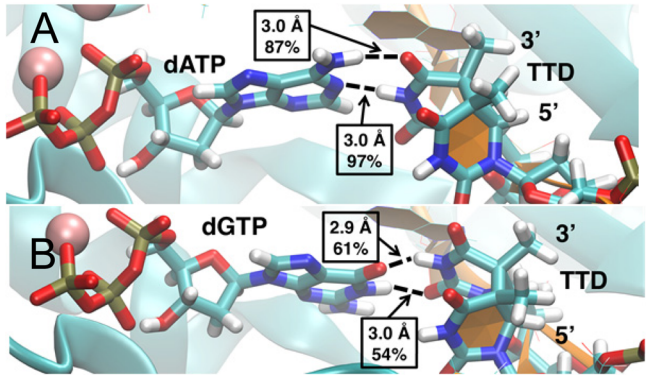

Figure 3. Base-pairing interactions of the dATP (A) and the dGTP (B) with the 3′ T of the TTD. Configurations were obtained from microsecond MD trajectories. The two hydrogen-bonding interactions are observed in significantly more configurations for the system with dATP than for the system with dGTP, indicating more persistent and stable base-pairing interactions for the system with dATP.

at these two positions was determined to be smaller with undamaged DNA.[8] Experimental studies have also shown higher processivity for the insertion of A opposite the 5′ T, which occurs after the incorporation of A opposite the 3′ T.[7,8,28] Our TI calculations for the AvsG5′ thermodynamic cycle (Scheme 1c) indicate that the relative binding free energy of dATP versus dGTP at the 5′T of the TTD is −2.9 ± 0.7 kcal/mol, again favoring dATP over dGTP binding. The data for the five independent TI calculations are provided in Table S4 and Figure S5. This calculated relative binding free energy is slightly more negative than the value calculated for the dATP versus dGTP binding at the 3′ position of the TTD and is consistent with the experimentally observed enhanced fidelity and processivity at the 5′ position, although the differences in the binding free energies are smaller than the error bars and thus are not statistically meaningful.

We did not observe significant differences between the dATP and dGTP hydrogen-bonding interactions with the enzyme at the 3′ T and at the 5′ T of the TTD in our previous analysis of microsecond MD trajectories.[22] However, again we find differences in the base-pairing interactions between the dNTP and the TTD. The most persistent hydrogen bonds between the dATP and the 5′ T of the TTD employ the same hydrogen-bonding partners on both molecules as in the previous case: 78% of all saved configurations display a hydrogen bond between the N1 of A and the N3 hydrogen of the 5′ T with an average donor−acceptor distance of 3.0 Å and a donor−hydrogen−acceptor angle of 152°, and 67% of all saved configurations display a hydrogen bond between one of the N6 hydrogens in A and the O4 atom of the 5′ T with an average donor−acceptor distance of 3.0 Å and a donor−hydrogen−acceptor angle of 161°. An advantage of the dATP insertion at the 5′ position arises from the additional hydrogen-bonding interactions that the TTD exhibits through the 3′ T, which already established A:T base pairing in the previous step of Pol η function. The same hydrogen-bonding partners in the 3′ T form two hydrogen bonds to the corresponding atoms in A at the 3′-end of the primer in 93% of the saved frames with a combined average donor−acceptor distance of 3.0 Å and an average donor−hydrogen−acceptor angle of 160°. Figure 4 depicts these A:T base-pairing interactions. These additional base-pairing interactions at the 3′ T hold the TTD more rigidly in place and hence could explain

DOI: 10.1021/jacs.5b08451
J. Am. Chem. Soc. 2015, 137, 13240−13243

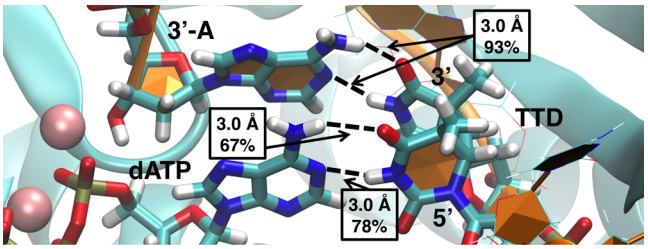

Figure 4. Base-pairing interactions between the dATP and the 5′ T of the TTD. The 3′ T of the TTD forms hydrogen bonds with the 3′-terminus of the DNA primer, which holds the TTD more rigidly compared to configurations in which the dATP binds at the 3′ T of the TTD (Figure 3A).

the experimentally observed higher fidelity and processivity for the insertion of A at the 5′ T compared to the 3′ T of the TTD.

Our calculations of the binding free energies are consistent with the experimental measurements of fidelity and processivity for Pol η. As summarized in Table 1, dATP binding to the enzyme−DNA complex is thermodynamically favored for TTD-containing DNA over undamaged DNA, and dATP binding is thermodynamically favored over dGTP binding at both the 3′ T and the 5′ T of the TTD, with a possible preference at the 5′ T. In addition, this analysis provides molecular level explanations for these differences in terms of hydrogen-bonding interactions between the TTD and the dATP or dGTP, as well as between the TTD and the enzyme. These insights have implications for drug design, particularly in efforts aimed at preventing the interference of Pol η with Pt-based cancer chemotherapy treatments. Specifically, understanding the nature of dNTP binding to the Pol η−DNA system could help guide the design of inhibitors of Pol η to block the translesion synthesis of DNA−Pt adducts.[10,12,32,33]

Table 1. Relative Binding Free Energies in kcal/mol, Obtained from the Presented Thermodynamic Cycles[a]

dATP to **TTD** vs TT	**dATP** vs dGTP to TTD at 3′ T	**dATP** vs dGTP to TTD at 5′ T
−4.3 ± 1.0	−2.4 ± 1.1	−2.9 ± 0.7

[a]The entity with favored binding is shown in bold.

■ ASSOCIATED CONTENT

Supporting Information

The Supporting Information is available free of charge on the ACS Publications website at DOI: 10.1021/jacs.5b08451.

Computational details of the TI calculations, tables displaying the results of replicate TI calculations for all cycles, plots pertaining to convergence of TI calculations, and complete ref 27(PDF)

■ AUTHOR INFORMATION

Corresponding Author

*shs3@illinois.edu

Notes

The authors declare no competing financial interest.

■ ACKNOWLEDGMENTS

This work was funded by National Institutes of Health grant GM056207. We thank Dr. A. V. Soudackov, Dr. J. W. Kaus, Dr. W. Yang, Dr. P. Hanoian, Dr. S. Gannavram, and Prof. S. Benkovic for helpful discussions. We acknowledge computing support from Extreme Science and Engineering Discovery Environment (XSEDE).

■ REFERENCES

(1) Lange, S. S.; Takata, K.; Wood, R. D. *Nat. Rev. Cancer* **2011**, *11*, 96.
(2) Yang, W. *Protein Sci.* **2011**, *20*, 1781.
(3) Masutani, C.; Kusumoto, R.; Yamada, A.; Dohmae, N.; Yokoi, M.; Yuasa, M.; Araki, M.; Iwai, S.; Takio, K.; Hanaoka, F. *Nature* **1999**, *399*, 700.
(4) Cruet-Hennequart, S.; Gallagher, K.; Sokol, A. M.; Villalan, S.; Prendergast, A. M.; Carty, M. P. *Subcell. Biochem.* **2010**, *50*, 189.
(5) Yang, W. *Biochemistry* **2014**, *53*, 2793.
(6) Yang, W.; Woodgate, R. *Proc. Natl. Acad. Sci. U. S. A.* **2007**, *104*, 15591.
(7) Kusumoto, R.; Masutani, C.; Shimmyo, S.; Iwai, S.; Hanaoka, F. *Genes Cells* **2004**, *9*, 1139.
(8) McCulloch, S. D.; Kokoska, R. J.; Masutani, C.; Iwai, S.; Hanaoka, F.; Kunkel, T. A. *Nature* **2004**, *428*, 97.
(9) Matsuda, T.; Bebenek, K.; Masutani, C.; Hanaoka, F.; Kunkel, T. A. *Nature* **2000**, *404*, 1011.
(10) Cruet-Hennequart, S.; Villalan, S.; Kaczmarczyk, A.; O'Meara, E.; Sokol, A. M.; Carty, M. P. *Cell Cycle* **2009**, *8*, 3043.
(11) Parsons, J. L.; Nicolay, N. H.; Sharma, R. A. *Antioxid. Redox Signaling* **2013**, *18*, 851.
(12) Ummat, A.; Rechkoblit, O.; Jain, R.; Choudhury, J. R.; Johnson, R. E.; Silverstein, T. D.; Buku, A.; Lone, S.; Prakash, L.; Prakash, S.; Aggarwal, A. K. *Nat. Struct. Mol. Biol.* **2012**, *19*, 628.
(13) Straatsma, T. P.; McCammon, J. A. *J. Chem. Phys.* **1991**, *95*, 1175.
(14) Deng, Y. Q.; Roux, B. *J. Phys. Chem. B* **2009**, *113*, 2234.
(15) Tembre, B. L.; McCammon, J. A. *Comput. Chem.* **1984**, *8*, 281.
(16) Gilson, M. K.; Zhou, H. X. *Annu. Rev. Biophys. Biomol. Struct.* **2007**, *36*, 21.
(17) Jorgensen, W. L. *Science* **2004**, *303*, 1813.
(18) Shirts, M. R.; Mobley, D. L.; Brown, S. P. In *Drug Design Structure- and Ligand-Based Approaches*; Merz, K. M., Ringe, D., Reynolds, C. H., Eds.; Cambridge University Press: New York, 2010; p 61.
(19) Michel, J.; Essex, J. W. *J. Comput.-Aided Mol. Des.* **2010**, *24*, 639.
(20) Christ, C. D.; Mark, A. E.; van Gunsteren, W. F. *J. Comput. Chem.* **2010**, *31*, 1569.
(21) The hydrogen bonds have a distance cutoff of 3.5 Å between the donor−acceptor atoms and an angle cutoff of 135° for the acceptor−hydrogen−donor angle.
(22) Ucisik, M. N.; Hammes-Schiffer, S. 2015, submitted.
(23) Lawrenz, M.; Baron, R.; McCammon, J. A. *J. Chem. Theory Comput.* **2009**, *5*, 1106.
(24) Steinbrecher, T.; Case, D. A.; Labahn, A. *Bioorg. Med. Chem.* **2012**, *20*, 3446.
(25) Genheden, S.; Nilsson, I.; Ryde, U. *J. Chem. Inf. Model.* **2011**, *51*, 947.
(26) Kaus, J. W.; Pierce, L. T.; Walker, R. C.; McCammon, J. A. *J. Chem. Theory Comput.* **2013**, *9*, 4131.
(27) Case, D. A.; et al. *AMBER 14*; University of California, San Francisco, 2014.
(28) Biertumpfel, C.; Zhao, Y.; Kondo, Y.; Ramon-Maiques, S.; Gregory, M.; Lee, J. Y.; Masutani, C.; Lehmann, A. R.; Hanaoka, F.; Yang, W. *Nature* **2010**, *465*, 1044.
(29) Masutani, C.; Kusumoto, R.; Iwai, S.; Hanaoka, F. *EMBO J.* **2000**, *19*, 3100.
(30) Johnson, R. E.; Washington, M. T.; Prakash, S.; Prakash, L. *J. Biol. Chem.* **2000**, *275*, 7447.
(31) Zhao, Y.; Gregory, M. T.; Biertumpfel, C.; Hua, Y. J.; Hanaoka, F.; Yang, W. *Proc. Natl. Acad. Sci. U. S. A.* **2013**, *110*, 8146.
(32) Alt, A.; Lammens, K.; Chiocchini, C.; Lammens, A.; Pieck, J. C.; Kuch, D.; Hopfner, K. P.; Carell, T. *Science* **2007**, *318*, 967.
(33) Zhao, Y.; Biertumpfel, C.; Gregory, M. T.; Hua, Y. J.; Hanaoka, F.; Yang, W. *Proc. Natl. Acad. Sci. U. S. A.* **2012**, *109*, 7269.

DOI: 10.1021/jacs.5b08451
J. Am. Chem. Soc. 2015, 137, 13240−13243